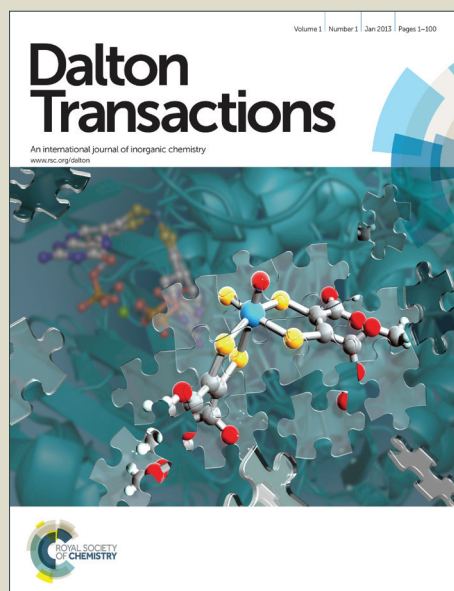


# Dalton Transactions

Accepted Manuscript

This article can be cited before page numbers have been issued, to do this please use: S. pouyamanesh, R. Tayebee, M. MOHAMMADPOUR AMINI and A. AliAkbari, *Dalton Trans.*, 2015, DOI:



This is an *Accepted Manuscript*, which has been through the Royal Society of Chemistry peer review process and has been accepted for publication.

*Accepted Manuscripts* are published online shortly after acceptance, before technical editing, formatting and proof reading. Using this free service, authors can make their results available to the community, in citable form, before we publish the edited article. We will replace this *Accepted Manuscript* with the edited and formatted *Advance Article* as soon as it is available.

You can find more information about *Accepted Manuscripts* in the [Information for Authors](#).

Please note that technical editing may introduce minor changes to the text and/or graphics, which may alter content. The journal's standard [Terms & Conditions](#) and the [Ethical guidelines](#) still apply. In no event shall the Royal Society of Chemistry be held responsible for any errors or omissions in this *Accepted Manuscript* or any consequences arising from the use of any information it contains.

## A new inorganic-organic hybrid material Al-SBA-15-TPI/H<sub>6</sub>P<sub>2</sub>W<sub>18</sub>O<sub>62</sub> catalyzed one-pot, three-component synthesis of 2H-Indazolo[2,1-b]phthalazine-triones

R. Tayebee<sup>a\*</sup>, M. M. Amini<sup>b</sup>, S. Pouyamanesh<sup>a</sup>, A. Aliakbari<sup>b</sup>

<sup>a</sup>Department of Chemistry, School of Sciences, Hakim Sabzevari University, Sabzevar 96179-76487, Iran

<sup>b</sup>Department of Chemistry, Shahid Beheshti University, G.C., Tehran 1983963113, Iran

### Abstract

A new inorganic-organic hybrid material Al-SBA-15-TPI/H<sub>6</sub>P<sub>2</sub>W<sub>18</sub>O<sub>62</sub> was prepared and was fully characterized by SEM, XRD, FT-IR, TGA-DTA, and UV-Vis spectroscopic techniques. Then, the prepared nanomaterial was used as a simple, cost-effective, and reusable heterogeneous catalyst for the synthesis of 2H-indazolo[2,1-b]phthalazine-1,6,11(13H)-trione derivatives by a one-pot, three-component condensation reaction of phthalhydrazide, cyclic diones, and aromatic aldehydes under solvent free conditions at 100 °C in a short time. This methodology proves to be efficient and environmentally benign in terms of high yields and low reaction times and offers significant improvements with regard to the scope of transformation and simplicity in operation by avoiding expensive or corrosive catalysts.

**Keywords:** Nanohybrid catalyst; H<sub>6</sub>P<sub>2</sub>W<sub>18</sub>O<sub>62</sub>; Phthalazine-triones; Heterogeneous.

### 1. Introduction

Study of hybrid organic-inorganic materials is an attractive prolific enterprise. Today fabrication, characterization, modification, and technological applications of organic-inorganic hybrid nanomaterials constitute an emerging prominent field in nanoscience and nanotechnology.<sup>1,2</sup> Synergism between hydrophobic and hydrophilic properties of the main components of hybrid materials exploited extraordinary properties and allow their applications in many fields. The design of novel hybrid nanocatalysts with new or improved properties has been the subject of attractive research fields in recent years.

Heterogenization of the heteropolyacids in an organic matrix and innovation of new organic-inorganic hybrid catalysts has been a recent trend in heterogeneous catalysis.<sup>3,4</sup> Therefore, hybridization of heteropolyacids offers new routes to generate well-defined,

\* Corresponding author: Reza Tayebee, Email: [Rtayebee@hsu.ac.ir](mailto:Rtayebee@hsu.ac.ir); Tel:+98-51-44410310; Fax: +98-51-44410300

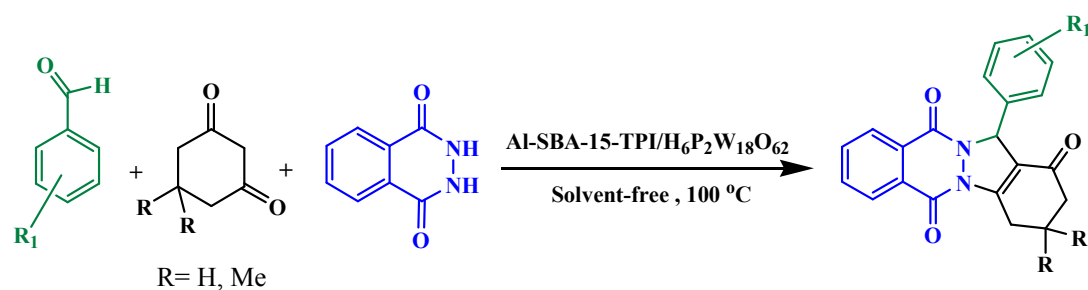
† Electronic supplementary information (ESI) is available.

functionalized molecular and supramolecular architectures through anchoring of heteropolyacids with an organic linker. Among different types of heteropolyacids, *Wells-Dawson* polytungsticacids are effective catalysts, which could be loaded on the surface of mesoporous materials such as SBA-15 to achieve a heterogeneous and reusable catalyst.

In the past few decades, heterocyclic chemistry has been one of the most profound disciplines in organic synthesis and pharmaceutical chemistry.<sup>5</sup> Heterocycles involving phthalazine moieties, which are capable to generate a bridgehead hydrazine, possess a wide range of implementations in pharmacology, such as anticonvulsant, vasorelaxant, and antitumor agent.<sup>6</sup> Moreover, fused phthalazines are effective envoys for inhibition of p38 MAP kinase, selective binding of GABA receptor, and as antianxiety drug.<sup>7</sup>

Although, different methods have been offered for preparation of phthalazine derivatives,<sup>8,9</sup> their broad utility range has accentuated the need to develop more efficient synthetic routes for the scaffold manipulation of phthalazine derivatives. Most protocols directed toward designing structural motifs containing phthalazine ring fragment, usually employ multi-component condensation of aldehydes and active methylene compounds such as malononitrile, ethyl cyanoacetate, and dimedone.<sup>10</sup> However, many of these protocols have their own limitations, such as use of expensive catalyst or toxic organic solvents, strong acidic conditions, and harsh reaction conditions. Moreover, considering importance of solvent-free organic reactions, new catalytic approaches should be taking into account for reduction of environmental wastes and energy cost. The possibility of performing multicomponent reactions under solvent free conditions with an efficient heterogeneous catalyst could enhance their efficacy from an economic as well as ecologic viewpoint.

In extension of our investigations to explore more effective catalysts in green organic synthesis by using simple and cost effective nanohybrid materials,<sup>11-13</sup> Al-SBA-15-TPI/H<sub>6</sub>P<sub>2</sub>W<sub>18</sub>O<sub>62</sub> as a new inorganic-organic hybrid material was prepared, characterized, and used as an efficient catalyst in the synthesis of 2H-indazolo[2,1-b] phthalazine-trione derivatives via one-pot, three-component condensation of phthalhydrazide, aromatic aldehydes, and dimedone under solvent free conditions (Scheme 1).



R<sub>1</sub>= electron withdrawing (donating), halogen, H

**Scheme 1** General formulation for the preparation of different phthalhydrazide-triones.

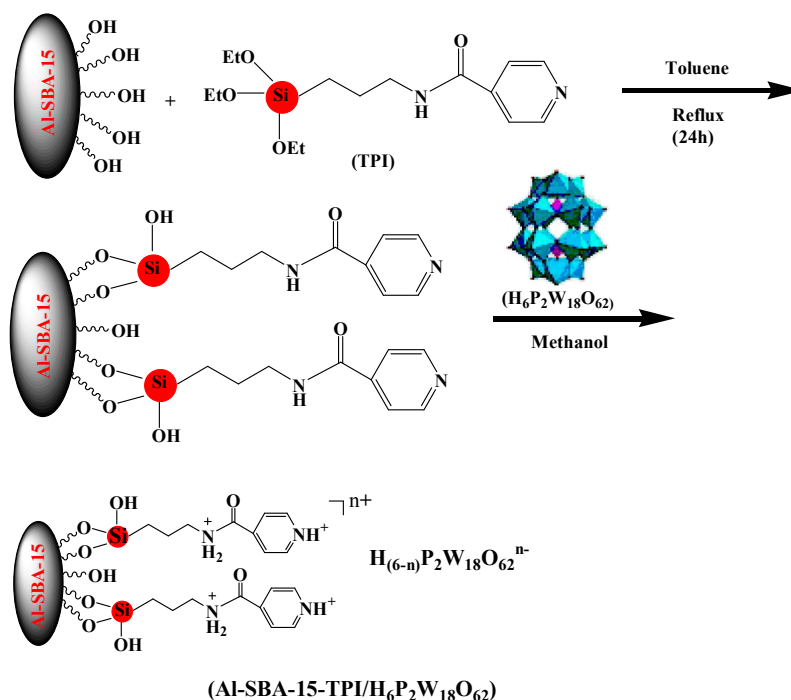
## 2. Experimental section

### 2.1. Materials and methods

All starting materials and solvents were obtained from commercial sources and used as received. Fresh aluminium tri-*sec*-butoxide (Al(O-<sup>*S*</sup>Bu)<sub>3</sub>) was prepared according to the literature procedure<sup>14</sup> and purified by vacuum distillation (167 °C/5 mmHg). Scanning electron microscope (SEM) micrographs were taken using a KYKY-EM3200 microscope (acceleration voltage 26 kV). The crystalline structures of the samples were evaluated by X-ray diffraction (XRD) analysis on a STOE diffractometer with Cu K<sub>α</sub> radiation ( $\lambda = 1.5418 \text{ \AA}$ ) at 40 keV and 40 mA with a scanning rate of  $3^\circ \text{ min}^{-1}$  in the  $2\theta$  range from 0.5 to  $80^\circ$ . Fourier transform infrared (FT-IR) spectra were recorded on a 8700 Shimadzu Fourier-Transform spectrophotometer in the region of 250 to  $4000 \text{ cm}^{-1}$  using KBr pellets. Thermogravimetric and differential thermal analysis (TGA-DTA) were carried out on a Bahr STA-503 instrument in air at a heating rate of  $10 \text{ }^\circ\text{C min}^{-1}$ . Ultraviolet-visible spectra were obtained on a Shimadzu Model UV-2550 spectrophotometer. Elemental analyses were performed with a Thermo Finnigan Flash-1112EA microanalyzer. Progress of the reactions was monitored by thin-layer chromatography (TLC). Melting points were recorded on a Bamstead electrothermal type 9200 melting point apparatus. <sup>1</sup>H and <sup>13</sup>C NMR spectra were recorded on a Bruker AVANCE 300-MHz instrument using TMS as internal reference. All products were identified by comparison of their spectral and physical data with those previously reported. *Wells-Dawson* H<sub>6</sub>P<sub>2</sub>W<sub>18</sub>O<sub>62</sub>·24H<sub>2</sub>O acid catalyst (HPA) was prepared according to the previously reported methods.<sup>15</sup> Synthesis of Al-SBA-15 and pyridine-functionalized Al-SBA-15-TPI are described in the supporting information.

## 2.2. Immobilization of *Wells-Dawson* diphosphooctadecatungstic acid on Al-SBA-15-TPI

For the immobilization of  $\text{H}_6\text{P}_2\text{W}_{18}\text{O}_{62} \cdot 24\text{H}_2\text{O}$  on Al-SBA-15-TPI, 50 ml of methanol containing 0.4 g of  $\text{H}_6\text{P}_2\text{W}_{18}\text{O}_{62} \cdot 24\text{H}_2\text{O}$  was added to a freshly prepared Al-SBA-15-TPI (0.8 g) and the mixture was refluxed for 4 h. Then, the heterogeneous catalyst was filtered off and washed with methanol several times and thereafter dried at room temperature. Amount of  $\text{H}_6\text{P}_2\text{W}_{18}\text{O}_{62} \cdot 24\text{H}_2\text{O}$  loading on Al-SBA-15-TPI was found to be 0.11 mmol/g, as determined by UV-Vis spectroscopy. This result was confirmed by thermogravimetric analysis. UV-Vis studies showed that 9.64% of pyridine groups on the surface of Al-SBA-15 were coordinated to the *Wells-Dawson* heteropolyacid. The functionalized Al-SBA-15-TPI/ $\text{H}_6\text{P}_2\text{W}_{18}\text{O}_{62}$  did not leach significantly after prolonged contact with aqueous solution, as confirmed by UV-Vis spectroscopy. Therefore, N-[3-(triethoxysilyl)propyl]isonicotinamide (TPI) linker was a suitable agent for the immobilization process and provided anchoring of the heteropolyacid onto the functionalized support. A schematic for the preparation of Al-SBA-15-TPI/HPA nanocatalyst is shown in Scheme 2.



**Scheme 2** A schematic for preparation of Al-SBA-15-TPI/HPA nanocatalyst.

### 2.3. General procedure for preparation of 2H-indazolo[2,1-b]phthalazine-1,6,11(13H)-triones

To a mixture of aldehyde (0.25 mmol), phthalhydrazide (0.25 mmol) and dimedone (0.25 mmol), Al-SBA-15-TPI/H<sub>6</sub>P<sub>2</sub>W<sub>18</sub>O<sub>62</sub> (0.02 g) was added and the mixture was heated to 100 °C for appropriate time. Completion of the reaction was monitored by TLC. After completion, hot ethanol (5 ml) was added to the reaction mixture and stirred for 5 min. Then, the heterogeneous solid catalyst was quickly filtered off and the filtrate was cold to 5 °C to precipitate the desired product. Finally, the solid product was further purified by recrystallization in aqueous EtOH (25%). The desired pure products were characterized by comparison of their physical data with those of known 2H-indazolo[2,1-b]phthalazine-1,6,11(13H)-triones.

### 2.4. Spectral data for some representative 2H-indazolo[1,2-b]phthalazine-1,6,11(13H)-triones<sup>36, 43</sup>

3,3-Dimethyl-13-phenyl-3,4-dihydro-2H-indazolo[2,1b]phthalazine-1,6,11(13H)-trione (Table 6, Entry 1): Yellow powder; m.p: 206-208 °C; IR (KBr) ( $\nu_{\max}$ , cm<sup>-1</sup>) 2956, 1665, 1574; <sup>1</sup>H NMR (300 MHz, CDCl<sub>3</sub>):  $\delta$  (ppm) 1.21 (s, 6H, 2Me), 2.33 (s, 2H, CH<sub>2</sub>C), 3.22-3.47 (AB system,  $J$  = 18.9 Hz, 2H, CH<sub>a</sub>H<sub>b</sub>CO), 6.44 (s, 1H, CHN), 7.29-8.36 (m, 9H, Ph); <sup>13</sup>C NMR (100 MHz, CDCl<sub>3</sub>):  $\delta$  (ppm) 28.3, 28.7, 34.8, 38.1, 50.9, 64.8, 118.7, 127.0-127.9, 128.6-129.1, 134.5, 136.4, 150.8, 154.2, 156.0, 192.1.

3,3-Dimethyl-13-(2-hydroxyphenyl)-3,4-dihydro-2H-indazolo[1,2-b]phthalazine-1,6,11(13H)-trione (Table 6, Entry 3): Yellow solid; m.p: 184-188 °C; IR (KBr,  $\nu_{\max}$  cm<sup>-1</sup>) 2897, 1661, 1492, 1378, 1328, 1262, 1082, 791. <sup>1</sup>H NMR (300 MHz, CDCl<sub>3</sub>):  $\delta$  (ppm) 10.98 (br s, 1H, OH), 8.25-8.34 (m, 2H), 7.83-7.85 (m, 2H), 6.97-7.56 (m, 4H, ArH), 6.33 (s, 1H, ArCH), 2.43 and 2.60 (AB-q system,  $J$  = 17.3 Hz, 2H), 2.32 (s, 2H), 1.03 (s, 3H, CH<sub>3</sub>), 0.97 (s, 3H, CH<sub>3</sub>); <sup>13</sup>C NMR (100 MHz, CDCl<sub>3</sub>):  $\delta$  (ppm) 201.1, 196.1, 169.3, 161.5, 150.8, 137.1, 133.4, 131.7, 128.7, 128.1, 127.5, 124.5, 120.6, 115.8, 111.1, 52.2, 43.3, 41.5, 27.3, 26.4.

3,3-Dimethyl-13-(3-nitrophenyl)-3,4-dihydro-2H-indazolo[1,2-b]phthalazine-1,6,11(13H)-trione (Table 6, Entry 4): Yellow powder; m.p: 268-271 °C; IR (KBr) ( $\nu_{\max}$ , cm<sup>-1</sup>) 2973, 1683, 1661, 1625; <sup>1</sup>H NMR (300 MHz, CDCl<sub>3</sub>):  $\delta$  (ppm) 1.23 (s, 6H, Me), 2.34 (s, 2H,

CH<sub>2</sub>C), 3.23-3.47 (AB system,  $J=18.9$  Hz, 2H, CH<sub>a</sub>H<sub>b</sub>CO), 6.53 (s, 1H, CHN), 7.54-8.4 (m, 8H, Ph); <sup>13</sup>C NMR (100 MHz, CDCl<sub>3</sub>):  $\delta$  (ppm) 28.4, 28.8, 34.8, 38.1, 50.8, 64.1, 117.2, 121.5, 123.8, 127.7, 128.1, 128.6, 128.9, 129.6, 133.9, 134.7, 138.4, 148.5, 150.7, 154.3, 155.9, 192.1.

13-(4-chlorophenyl)-3,3-Dimethyl-3,4-dihydro-2H-indazolo[1,2-b]phthalazine-1,6,11(13H)-trione (Table 6, Entry 7): Yellow powder; m.p: 262-264 °C; IR (KBr) ( $\nu_{\max}$ , cm<sup>-1</sup>) 2957, 2931, 1688, 1654, 1622; <sup>1</sup>H NMR (300 MHz, CDCl<sub>3</sub>):  $\delta$  (ppm) 1.22 (s, 6H, 2Me), 2.33 (s, 2H, CH<sub>2</sub>C), 3.22-3.44 (AB system,  $J=19.2$  Hz, 2H, CH<sub>a</sub>H<sub>b</sub>CO), 6.41 (s, 1H, CHN), 7.28-7.38 (dd,  $J=8.4$  Hz, 4H, ArCl), 7.84-8.38 (m, 4H, Ph); <sup>13</sup>C NMR (100 MHz, CDCl<sub>3</sub>):  $\delta$  (ppm) 28.5, 28.7, 34.7, 38.0, 50.9, 64.31, 118.5, 127.1, 127.7, 127.8, 128.6, 128.6, 128.8, 129.1, 133.4, 134.5, 136.3, 150.8, 154.4, 156.0, 192.2.

3,3-Dimethyl-13-(4-methylphenyl)-3,4-dihydro-2H-indazolo[2,1-b]phthalazine-1,6,11(13H)-trione (Table 6, Entry 15): Yellow powder; m.p: 226-228 °C ; IR (KBr) ( $\nu_{\max}$ , cm<sup>-1</sup>) 2958, 1667, 1631; <sup>1</sup>H NMR (300 MHz, CDCl<sub>3</sub>):  $\delta$  (ppm) 1.21 (s, 6H, 2Me), 2.20 (s, 3H, CH<sub>3</sub>), 2.33 (s, 2H, CH<sub>2</sub>C), 3.21-3.45 (AB system,  $J=18.9$  Hz, 2H, CH<sub>a</sub>H<sub>b</sub>CO), 6.43 (s, 1H, CHN), 7.12-7.32 (dd,  $J=7.8$  Hz, 4H, ArMe) 7.83-8.36 (m, 4H, Ph); <sup>13</sup>C NMR (100 MHz, CDCl<sub>3</sub>):  $\delta$  (ppm) 21.3, 28.4, 28.6, 34.6, 38.1, 50.9, 64.7, 118.7, 127.1, 127.7, 128.9, 129.1, 129.4, 133.4, 134.4, 138.3, 148.5, 150.7, 154.1, 156.1, 192.1.

13-isobutyl-3,3-Dimethyl-3,4-dihydro-1H-indazolo[1,2-b]phthalazine-1,6,11(2H,13H)-trione (Table 6, Entry 16): Yellow powder; m.p: 135-137 °C; IR (KBr) ( $\nu_{\max}$ , cm<sup>-1</sup>) 2959, 2872, 1663, 1631; <sup>1</sup>H NMR (300 MHz, CDCl<sub>3</sub>):  $\delta$  (ppm) 0.86-0.87 (d, 3H, Me), 0.94 (d, 3H, Me), 1.21 (s, 3H, Me), 1.25 (s, 3H, Me), 1.68-1.75 (m, 1H, CH), 2.01-2.05 (m, 1H, CH), 2.14-2.18 (m, 1H, CH), 2.35-2.45 (AB system,  $J=15$  Hz, 2H), 3.14-3.35 (AB system,  $J=19$  Hz, 2H), 5.7 (m, 1H, CHN), 7.85-7.93 (m, 2H, Ph), 8.34-8.38 (m, 2H, Ph); <sup>13</sup>C NMR (100 MHz, CDCl<sub>3</sub>):  $\delta$  (ppm) 23.1, 24.1, 25.3, 28.8, 29.0, 34.8, 38.5, 39.8, 51.5, 62.2, 118.7, 127.8, 128.3, 129.8, 129.4, 133.8, 134.8, 151.7, 155.3, 156.5, 193.3.

### 3. Results and discussion

Organic-inorganic hybrid silica-based porous materials have been extensively contemplated, because of their glamorous properties such as regular mesostructure, thermal and mechanical stability, tuneable pore size, high adsorption capacity, as well as extraordinarily wide possibilities of functionalization with organic linkers.<sup>16,17</sup> Therefore, development of porous

silica-based materials with large specific surface areas is currently an area of extensive research, particularly with regard to potential applications in areas such as adsorption, chromatography, catalysis, sensor technology, and gas storage.

In spite of good catalytic applications reported for hybrid materials composed of SBA-15, its surface acidity is not sufficient and introducing metal ions, such as aluminium, in the neutral silica framework, directed to generation of more surface acidic sites.<sup>18</sup> Generally, incorporation of heteroatoms, such as aluminium, into the mesoporous materials introduces a charge imbalance in the framework which is balanced by protons, thus generating bridging hydroxyl groups (Si-OH-Al, as *Bronsted* acidic sites) on the surface of these materials.<sup>19</sup> Among the metal-substituted mesoporous materials, aluminium incorporated mesoporous silicas have great potential in moderate acid catalyzed reactions for large molecules.<sup>20</sup> There are different strategies for the direct synthesis of aluminium-substituted mesoporous silica under acidic conditions.<sup>20</sup> Prehydrolysis of the alkoxysilanes before addition of aluminium alkoxide, is generally more utilized. In this strategy, aluminium tri-*sec*-butoxide is used as the aluminium source, and hydrolyzed rapidly to monomeric  $\text{Al}(\text{OH})_4^-$  under acidic or basic conditions. Hydrolysis of aluminium tri-*sec*-butoxide under high acidic conditions, resulted in formation of soluble tetrahedral coordinated aluminium precursors, which favour incorporation of aluminium into the mesoporous materials.

### 3.1. Structural characterization of Al-SBA-15-TPI/HPA nanocatalyst

#### 3.1.1. X-ray diffraction (XRD) studies

Low-angle X-ray diffraction patterns of Al-SBA-15, Al-SBA-15-TPI, and Al-SBA-15-TPI/HPA are shown in Fig. S1†. All patterns present a very intense peak at  $2\theta \sim 0.9^\circ$  which can be indexed to the (100) hkl reflection. This peak is associated with the  $P6mm$  hexagonal symmetry typical of SBA-15 material and indicating a significant degree of long-range ordering in the structure and a well-formed hexagonal lattice.<sup>21</sup> Diffraction patterns indicated that the primary structure of Al-SBA-15 was maintained after modification with TPI and anchoring with the heteropolyacid. Due to the grafting of pyridine groups, the diffraction peak of Al-SBA-15 was slightly shifted to higher angle and became weaker compared with that of the unmodified one. These results indicated that the mesoporous phase of the composite was maintained, while integrity of the mesopore structure was affected by the incorporation of TPI as functionalizing agent.<sup>22</sup> A slight shift of the characteristic reflection of Al-SBA-15-TPI/HPA in the low-angle XRD pattern indicated that  $\text{H}_6\text{P}_2\text{W}_{18}\text{O}_{62}$  mostly

occupied mesoporous channels.<sup>23</sup> HPA loading induced a striking effect on the width and intensity of the main reflection at  $d_{100}$  spacing and this line became broader and weaker with a marginal shift indicating a noticeable decrease in the order of Al-SBA-15 and occupation of the mesopore channels with  $H_6P_2W_{18}O_{62}$ .<sup>24</sup> Bulk HPA crystal phase did not appear in the HPA supported Al-SBA-15-TPI material, indicating that HPA was finely dispersed on the surface of Al-SBA-15-TPI. Furthermore, the high-angle XRD pattern of  $H_6P_2W_{18}O_{62}$  immobilized on Al-SBA-15-TPI showed that  $H_6P_2W_{18}O_{62}$  diffraction peaks were collapsed and only a broad peak was observed at  $2\theta$  about  $22^\circ$  after incorporation with the functionalized support. This finding confirmed that the heteropolyacid was well dispersed onto the Al-SBA-15 mesopore. This is in agreement with the XRD pattern of other heteropolyacids used in other supports.<sup>25</sup>

### 3. 1. 2. UV-Vis spectroscopy

UV-Vis spectrum of the *Wells–Dawson* heteropolyacid showed two types of ligand→metal charge-transfer bands originating from different oxygen atoms.<sup>26</sup> The highest energy absorption band at about 220 nm was assigned to  $O_d \rightarrow W$  charge-transfer band due to the terminal oxygen atoms. Other weak bands at ~260 and ~310 nm are characteristic bands for diphosphooctadecatungstic acid and are attributed to the  $O_b \rightarrow W$  or  $O_c \rightarrow W$  charge-transfer bands originating from the bridging oxygen atoms.

To determine the extent of HPA which can be loaded on the support, 0.8 g of Al-SBA-TPI was suspended in a 50 ml methanol solution of HPA with an initial concentration 8000 ppm. The suspension was refluxed for 4 h; absorption spectrum was recorded for the solution after removing the solid catalyst by filtration (Fig. 1). After 240 min refluxing and comparison with the standard solutions, the heteropolyacid concentration had declined to 250 ppm which corresponded to  $0.11 \text{ mmol g}^{-1}$  loading of HPA on the support.

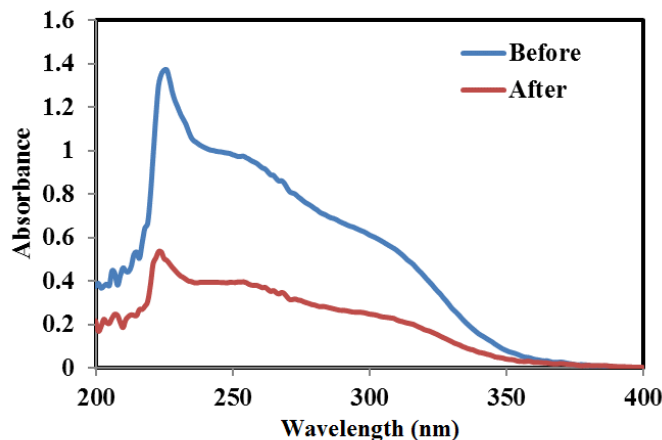


**Fig. 1** UV-Vis spectral changes after addition of  $\text{H}_6\text{P}_2\text{W}_{18}\text{O}_{62}$  to Al-SBA-15-TPI under reflux for 4 h.

### 3. 1. 3. Studying morphology (SEM) of Al-SBA-15-TPI/HPA nanocatalyst

Morphology of Al-SBA-15-TPI/HPA nanocatalyst was investigated by SEM (Fig. 2). The spherical-elliptical particles in this micrograph are attributed to Al-SBA-15-TPI/HPA. Actually, by introducing aluminium into the silica, the robe-like morphology, which is consistent with known SBA-15 structure, was changed to some extent. However, functionalization with *N*-(3-(triethoxysilyl) propyl) isonicotinamide and anchoring HPA had no significant effect on the structure of pure Al-SBA-15.

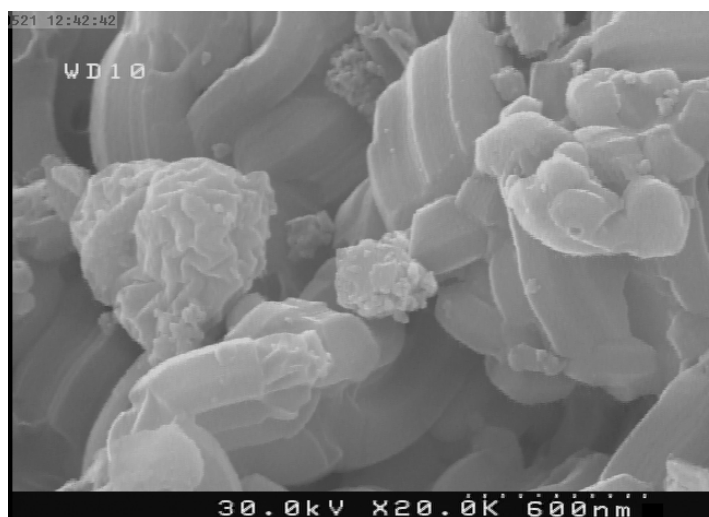


**Fig. 2** SEM micrograph of the Al-SBA-15-TPI/HPA nanocatalyst.

### 3. 1. 4. FT-IR spectroscopy

To ascertain covalent binding of TPI and anchoring of HPA into the surface of Al-SBA-15 mesopores, FT-IR spectroscopy was used for characterization of the ordered mesoporous Al-SBA-15, Al-SBA-15-TPI, and Al-SBA-15-TPI/HPA (Fig. 3). TPI was attached to the surface of SBA-15 by condensation of the silanol groups of alumina-silica and the ethoxy groups of TPI under refluxing in toluene. Presence of organic groups is confirmed by observation of C-H aromatic, C-H aliphatic, C=O, and C=N groups around 3050, 2800-2950, 2652, 1650 and 1550  $\text{cm}^{-1}$  region, respectively. Broad N-H stretching bands were superimposed to those of water, in the 3000–3500  $\text{cm}^{-1}$  range.<sup>27</sup> These findings proved that pyridine groups have been successfully grafted to the surface of Al-SBA-15. Furthermore, FT-IR spectra of Al-SBA-15, Al-SBA-15-TPI, and Al-SBA-15-TPI/HPA revealed the typical Si-O-Si bands of the inorganic framework; symmetric stretching vibration mode around 800  $\text{cm}^{-1}$  and asymmetric stretching vibration around 1080–1100  $\text{cm}^{-1}$ .<sup>28</sup>

The absorption peak of the Si-OH bands at 960  $\text{cm}^{-1}$  in Al-SBA-15 weaken upon functionalization, indicating that the TPI agents are substituted with some of the surface silanol groups. The broad band in 3000–3700  $\text{cm}^{-1}$  region and the band at 1630-1650  $\text{cm}^{-1}$  can be attributed to the symmetrical stretching and bending vibrations of the adsorbed water molecules, respectively. In comparison with the pure SBA-15, there is a slight shift toward higher frequencies for the bands in which attributed to Si-O-Si, as a result of longer Al-O bond distance than Si-O.

*Wells–Dawson* structure of  $\text{H}_6\text{P}_2\text{W}_{18}\text{O}_{62}$  consists of two half units composed of a central  $\text{PO}_4$  tetrahedron surrounded by nine  $\text{WO}_6$  octahedral. Therefore, the  $\text{H}_6\text{P}_2\text{W}_{18}\text{O}_{62}$  structure involves four kinds of oxygen atoms. The first is  $\text{P-O}_a$  in which the oxygen atom connects with the tungsten atoms, the second is  $\text{W-O}_b\text{-W}$  oxygen bridges (corner-sharing oxygen bridges between different  $\text{W}_3\text{O}_{13}$  groups), the third is  $\text{W-O}_c\text{-W}$  oxygen bridges (edge-sharing oxygen bridge within  $\text{W}_3\text{O}_{13}$  groups), and the last is  $\text{W-O}_d$  terminal oxygen atoms. The four characteristic bands of  $\text{H}_6\text{P}_2\text{W}_{18}\text{O}_{62}$  were appeared at  $\nu_{\text{as}}(\text{W-O}_d)$ : 965  $\text{cm}^{-1}$ ;  $\nu_{\text{as}}(\text{W-O}_b\text{-W})$ : 912  $\text{cm}^{-1}$ ;  $\nu_{\text{as}}(\text{W-O}_c\text{-W})$ : 776  $\text{cm}^{-1}$  and  $\nu_{\text{as}}(\text{P-O}_a)$ : 1093  $\text{cm}^{-1}$ .<sup>29</sup>

In the FT-IR spectrum of Al-SBA-15-TPI/HPA observation of HPA was hindered as a result of the strong background of alumina-silica support. Actually, from four characteristic bands of HPA,  $\text{W-O}_c\text{-W}$  and  $\text{P-O}_a$  bands overlap with those of Si-O-Si stretching vibrations

of mesoporous supports and only the bands corresponding to  $W-O_d$  ( $961\text{ cm}^{-1}$ ) and  $W-O_b-W$  ( $914\text{ cm}^{-1}$ ) were discernable after immobilization. Appearance of HPA characteristic bands in the FT-IR spectrum of Al-SBA-15-TPI/HPA revealed that the *Well-Dawson* structure remained intact after immobilization.

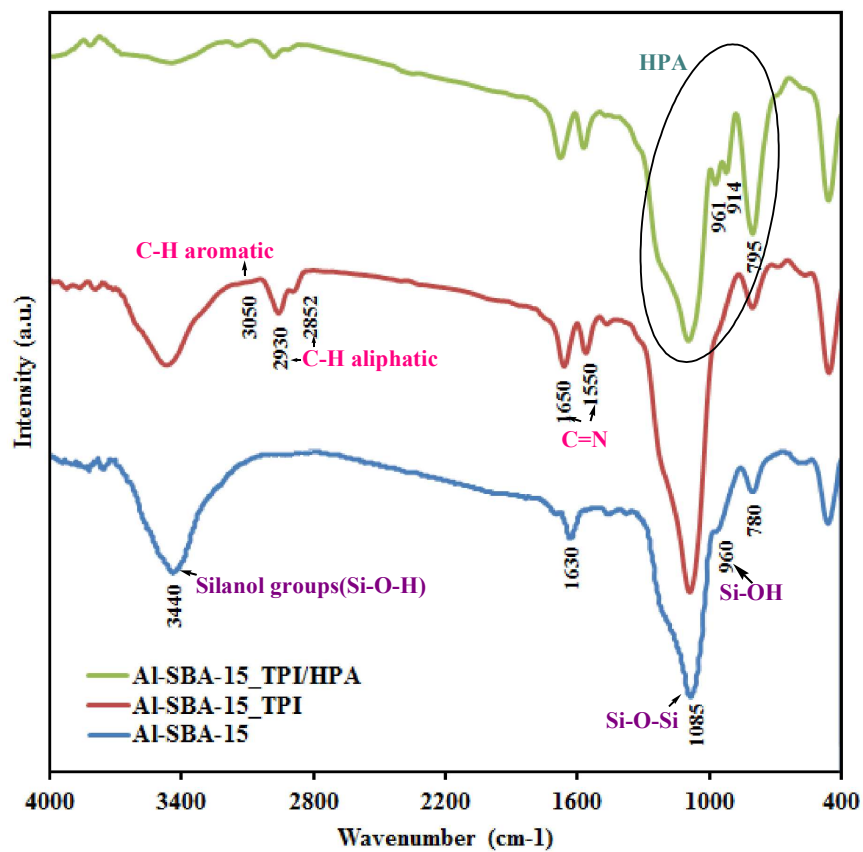
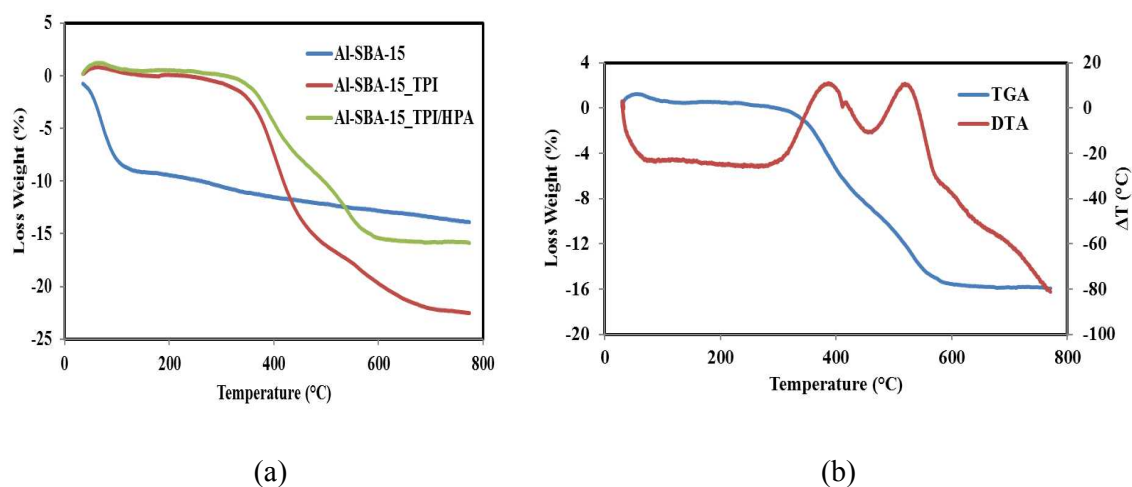


Fig. 3 FT-IR spectra of Al-SBA-15, Al-SBA-15-TPI, and Al-SBA-15-TPI/HPA.

### 3. 1. 5. Thermal analysis

The thermal stability of Al-SBA-15 support, Al-SBA-15-TPI, and Al-SBA-15-TPI/HPA nanocatalyst were investigated by carrying out TGA analysis (Fig. 4a). Moreover, the thermal stability of Al-SBA-15-TPI/HPA nanocatalyst was investigated by carrying out TGA–DTA analysis (Fig. 4b). TGA curve of alumina-silica support contains two steps of weight loss. The first weight loss (~9%) in the temperature range of 25–125 °C which is accompanied with endothermic peaks in DTA curve was attributed to the release of physically adsorbed water and the second one (3.5%) in the range of 125–800 °C was due to the dehydroxylation

of OH groups. TGA profile of Al-SBA-15-TPI and Al-SBA-15-TPI/HPA both showed a weight loss of 23 and 16%, respectively. This occurred in the temperature range of 300-800 °C, which is accompanied by a broad exothermic peak between 370 °C and 510 °C in the DTA curve (Fig. 4b), corresponding to the combustion of the organic part of TPI. The 23% weight loss in Al-SBA-15-TPI gave TPI concentration as 1.14 mmol/g in the alumina-silica mesopore which was in agreement with CHN analysis.



**Fig. 4** (a) TGA curves of Al-SBA-15, Al-SBA-15-TPI, and Al-SBA-15-TPI/HPA. (b) TGA and DTA of Al-SBA-15-TPI/HPA.

Although the apparent thermogram curves of Al-SBA-15-TPI and Al-SBA-15-TPI/HPA are similar, the amount of weight loss is higher for pyridine functionalized alumina-silica mesopore. Indeed, the presence of heteropolyacid, which was retained intact at the high temperature on Al-SBA-15-TPI, decreased organic moiety percentage on the resulting nanocatalyst, so the amount of weight loss is declined in HPA anchored mesopore compared to Al-SBA-15-TPI. Furthermore, according to thermal analysis, the prepared nanocatalyst was stable up to 300 °C.

### 3. 2. Catalytic tests

Multi-component reactions (MCRs) have attracted extensive interest in organic syntheses and in pharmaceutical chemistry. This strategy has provided more facile, fast, atom efficient and environmentally benign processes by mixing different starting materials in a single step and

avoiding the complicated isolation and purification of intermediates.<sup>30</sup> Therefore, MCRs have been considered as a practical, economic, and green approach to access diverse structures of complex products. Now, the catalytic activity of new heteropolyacid based inorganic-organic nanonano hybrid catalyst Al-SBA-15-TPI/H<sub>6</sub>P<sub>2</sub>W<sub>18</sub>O<sub>62</sub> is assessed for the preparation of 2H-indazolo[2,1-b]phthalazine-1,6,11(13H)-triones under heterogeneous solvent free conditions.

### 3. 2. 1. Effect of the heteropolyacid nature and structure on the efficacy of the catalytic system

Catalytic activity of H<sub>6</sub>P<sub>2</sub>W<sub>18</sub>O<sub>62</sub> was compared with other indicative familiar heteropolyacids in the preparation of 2,2-dimethyl-13-phenyl-2,3-dihydro-1H-indazolo[2,1-b]phthalazine-4,6,11(13H)-trione (Table 1). Almost, all the introduced *Keggin* and *Wells-Dawson* heteropolyacids are strong acids and behaved as good catalysts in the respective transformation.<sup>31</sup> Although, *Keggin*-type heteropolyacids have shown better catalytic activity than *Wells-Dawson* counterparts in many acid catalyzed organic transformations, however, *Wells-Dawson* type polytungstic acid H<sub>6</sub>P<sub>2</sub>W<sub>18</sub>O<sub>62</sub> clearly showed higher reactivity in the preparation of phthalazine-trione derivatives. Many factors such as acidity of the heteropolyacid, negative charge density smeared over oxygen atoms, structural composition and distortions, and absorption of the substrate molecule into the bulk of the heteropolyacid would contribute to the catalytic efficiency of the heteropolyacids under the reaction conditions.<sup>31</sup>

**Table 1** Effect of the heteropolyacid nature and structure on the efficacy of the preparation of 2,2-dimethyl-13-phenyl-2,3-dihydro-1H-indazolo[2,1-b]phthalazine-4,6,11(13H)-trione

Catalyst	Structure type	Time (min)	Yield (%)
H <sub>3</sub> PMo <sub>12</sub> O <sub>40</sub>	<i>Keggin</i>	25	60
H <sub>3</sub> PW <sub>12</sub> O <sub>40</sub>	<i>Keggin</i>	20	81
H <sub>6</sub> P <sub>2</sub> W <sub>18</sub> O <sub>62</sub>	<i>Wells-Dawson</i>	10	86
H <sub>6</sub> P <sub>2</sub> Mo <sub>18</sub> O <sub>62</sub>	<i>Wells-Dawson</i>	25	73
H <sub>4</sub> SiW <sub>12</sub> O <sub>40</sub>	Si-substituted <i>Keggin</i>	20	50
H <sub>4</sub> SiW <sub>9</sub> Mo <sub>2</sub> O <sub>40</sub>	Si-substituted mixed metal <i>Keggin</i>	25	78
H <sub>4</sub> SiW <sub>9</sub> Mo <sub>3</sub> O <sub>40</sub>	Si-substituted mixed metal <i>Keggin</i>	35	80

$H_{14}NaP_5W_{30}O_{110}$  Preyssler

20

68

To a mixture of aldehyde (0.25 mmol), phthalhydrazide (0.25 mmol) and dimedone (0.25 mmol), catalyst (0.75 mol%) was added and the mixture was heated to 100 °C for the required time. Progress of the reaction was monitored with TLC. Work-up was carried out as described in the experimental section. Yield% refers to the isolated yield.

### 3. 2. 2. Effect of catalyst amount on the catalytic efficiency

In next step, a study set out to determine the optimal amount of  $H_6P_2W_{18}O_{62}$  and Al-SBA-15-TPI/ $H_6P_2W_{18}O_{62}$  in the preparation of 2,2-dimethyl-13-phenyl-2,3-dihydro-1H-indazolo[2,1-b]phthalazine-4,6,11(13H)-trione. Therefore, the reaction was carried out by varying amount of the catalyst (Table 2). Maximum yield of 86% was attained with 0.75 mol% (0.033 g) of  $H_6P_2W_{18}O_{62}$  after 10 min; whereas, only 0.021 g of the nanocatalyst Al-SBA-15-TPI/ $H_6P_2W_{18}O_{62}$  (involving 0.224 mol% of  $H_6P_2W_{18}O_{62}$ ) led to 82% yield after a very short period of time of time (5 min). Clearly, Al-SBA-15-TPI/ $H_6P_2W_{18}O_{62}$  was more effective than  $H_6P_2W_{18}O_{62}$  and fewer amount of the heteropolyacid was needed to reach the maximum yield in a very short reaction time. Moreover, further increase in the amount of the catalyst in the aforementioned reaction did not a significant effect on the product yield and reaction time.

**Table 2** Effect of the catalyst amount on the condensation of benzaldehyde, phthalhydrazide, and dimedone under solvent-free conditions

Entry	Al-SBA-15-TPI/ $H_6P_2W_{18}O_{62}$ (g)	$H_6P_2W_{18}O_{62}$ (mol%)	Time (min)	Yield (%)
1	0	0	120	21
2	0.007	0.074	5	72
3	0.010	0.112	5	75
4	0.014	0.149	5	78
5	0.021	0.224	5	82
6	-	0.75	10	86

General reaction conditions are as described below Table 1.

### 3. 2. 3 Effect of reaction time on the catalytic efficiency

Effect of reaction time was also investigated to explore minimum time required to obtain the maximum yield in the preparation of 2,2-dimethyl-13-phenyl-2,3-dihydro-1H-indazolo[2,1-b]phthalazine-4,6,11(13H)-trione catalyzed by  $H_6P_2W_{18}O_{62}$  (0.75 mol%). As illustrated in Fig. S2†, only 5 min is sufficient to get 84% yield. No obvious increase in yield% was detected after a prolonged reaction time. However, a slight decrease was observed after 15 min.

### 3. 3. Studying catalytic efficiency of different (support-organic linker/heteropolyacid) hybrid materials

Several reports declared that electrostatic attachment of heteropolyacids to the solid supporting materials via a suitable linker is a beneficial strategy to overcome leaching of the catalytically active catalyst from the surface of supporting material. Thus, effect of the kind and nature of some organic modifiers, as linkers between solid supporting material and the heteropolyacid, was studied in this research. Results revealed that these organic linkers significantly affected the catalytic efficiency of  $H_5PW_{10}V_2O_{40}$  (Table 3). Mesoporous silica SBA-15 with the well-ordered hexagonal arrays of cylindrical channels, and a large number of silanol groups at the surface,<sup>32</sup> was served as an intriguing support for this study. This material led to much better results than  $Fe_3O_4$  in this study.

**Table 3** Effect of different organic linkers on the catalytic efficiency.

Catalyst	Amount (g)	Time (min)	Yield (%)	Ref.
SBA-15-pip- $H_5PW_{10}V_2O_{40}$	0.005	10	73	23
Al-SBA-15- TPI/ $H_6P_2W_{18}O_{62}$	0.01	5	78	this work
$Fe_3O_4$ - TPI/ $H_5PW_{10}V_2O_{40}$	0.01	20	34	4
$Fe_3O_4$ - TPI/ $H_6P_2W_{18}O_{62}$	0.01	20	36	26
Al-SBA-15	0.01	25	70	this work
SBA-15	0.01	35	57	32

General reaction conditions are as described below Table 1. All reactions were carried out at 100 °C.

Effects of the kind of solid support material, organic linker, and the catalytically active heteropolyacid on the efficacy of the prepared inorganic-organic hybrid material are also shown in Table 3. MCM-41 mesoporous silica was obviously more effective than  $\text{Fe}_3\text{O}_4$  as the solid support. MCM-41- $\text{NH}_2\text{-H}_5\text{PW}_{10}\text{V}_2\text{O}_{40}$  led to 86% yield after 20 min; whereas, the  $\text{Fe}_3\text{O}_4$  counterpart produced only 33% of product during the same time and under similar conditions. Moreover, nature of the organic linker was ineffective in  $\text{Fe}_3\text{O}_4$ -linker- $\text{H}_5\text{PW}_{10}\text{V}_2\text{O}_{40}$ . Both  $\text{Fe}_3\text{O}_4\text{-NH}_2\text{-H}_5\text{PW}_{10}\text{V}_2\text{O}_{40}$  and  $\text{Fe}_3\text{O}_4\text{-TPI-H}_5\text{PW}_{10}\text{V}_2\text{O}_{40}$  led to ~33% yield after 20 min. However, the *Wells-Dawson*  $\text{H}_6\text{P}_2\text{W}_{18}\text{O}_{62}$  was substantially more effective than the *Keggin* vanadium substituted  $\text{H}_5\text{PW}_{10}\text{V}_2\text{O}_{40}$ . Carbon nanotube modified with TPI was also used as the supporting material. Although, this new heterogeneous catalyst attracted the interest of several research groups, however, it was significantly less effective than the target heterogeneous catalyst used in this study, Al-SBA-15-TPI- $\text{H}_6\text{P}_2\text{W}_{18}\text{O}_{62}$ .

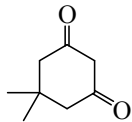
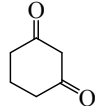
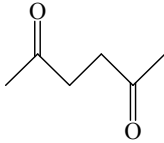
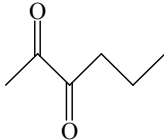
The catalytic activity of the ingredients comprising the organic–inorganic nanohybrid material Al-SBA-15-TPI/ $\text{H}_6\text{P}_2\text{W}_{18}\text{O}_{62}$  was investigated. Results showed that incorporation of 15% aluminum into the framework of SBA-15 significantly increased efficacy of the supporting material. 0.01 g of SBA-15 produced 57% yield after 35 min; whereas, the same amount of Al-SBA-15 led to 70% yield after 25 min. Moreover, anchoring of the *Wells-Dawson*  $\text{H}_6\text{P}_2\text{W}_{18}\text{O}_{62}$  to the modified Al-SBA-15 led to 78% yield after 5 min. Clearly, the new synthesized nanohybrid material Al-SBA-15-TPI/ $\text{H}_6\text{P}_2\text{W}_{18}\text{O}_{62}$  behaved as a unique and effective catalyst in the desired condensation reaction.

### 3. 4. Studying condensation of phthalhydrazide and aromatic aldehydes with different diketones

To further explore the scope of this protocol, we decided to investigate condensation reaction of phthalhydrazide and aromatic aldehydes with other cyclic and acyclic diketones in the presence of Al-SBA-15-TPI/ $\text{H}_6\text{P}_2\text{W}_{18}\text{O}_{62}$  (0.02 g). Among the examined diketones (Table 4), dimedone, 5,5-dimethyl-1,3-cyclohexane-dione, led to the best yield%; whereas, the unsubstituted 1,3-cyclohexane-dione was less effective. Cyclohexane-1,3-dione afforded the corresponding condensation product with 74% yield after 15 min. It seems that electron releasing nature of the two methyl substituents in dimedone would activate the diketone

toward condensation reaction. Two linear hexane diones, *i.e.* 2, 5-hexane-dione and 2, 3-hexane-dione were also tested. Obviously, linear diones were clearly less effective than the cyclic ones and both linear hexane diones led to 38-43% yield after 45-50 min; whereas, the cyclic diones provided 74-82% of products after shorter times 5-15 min.

**Table 4** Studying reactivity of cyclic and linear hexanediones towards the desired condensation reaction.

Diketone	Structure	Time (min)	Yield (%)
5,5-dimethyl-1,3-cyclohexane-dione		5	82
1,3-cyclohexane-dione		15	74
2,5-hexane-dione		50	38
2,3-hexane-dione		45	43

General reaction conditions are as described below Table 1.

### 3. 5. Comparison of the catalytic activity of Al-SBA-15-TPI/H<sub>6</sub>P<sub>2</sub>W<sub>18</sub>O<sub>62</sub> nanocatalyst with some reported catalysts

Comparison of the efficacy of Al-SBA-15-TPI/H<sub>6</sub>P<sub>2</sub>W<sub>18</sub>O<sub>62</sub> catalyst with some reported catalysts in the literature is presented in Table 5. The model reaction of dimedone, phthalhydrazide, and benzaldehyde was considered as a representative example and the comparison was in terms of mol% or amount of the catalyst, temperature, reaction time, and

percentage yields. Obviously, the present new nanohybrid catalyst (Al-SBA-15-TPI/H<sub>6</sub>P<sub>2</sub>W<sub>18</sub>O<sub>62</sub>) was more effective than most of the conventional catalysts listed in Table 5. The present methodology utilized a very low amount of the heterogeneous catalyst under solvent-free conditions. Although, some of the introduced additives catalyzed the reaction, even though at a lower temperature, they required toxic and expensive solvents, higher mol% of catalyst, and longer reaction times.

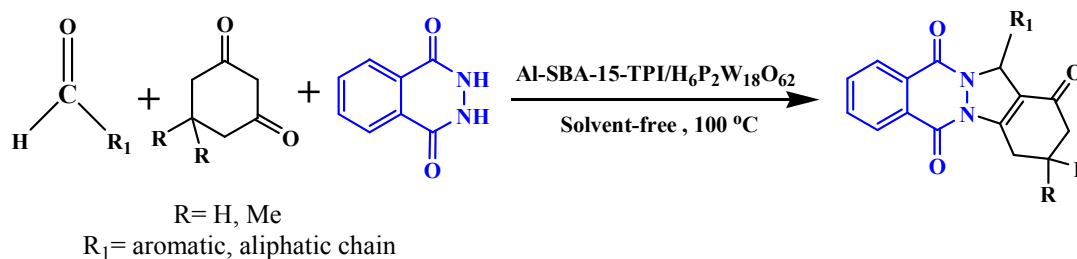
**Table 5** Comparison of the catalytic efficiency of Al-SBA-15-TPI/H<sub>6</sub>P<sub>2</sub>W<sub>18</sub>O<sub>62</sub> nanocatalyst with some reported catalysts.

Entry	Catalyst and Conditions	Time (min)	Yield (%)	Ref.
1	PSA, Solvent free, 100 °C, 7 mol%	10	91	33
2	H <sub>4</sub> SiW <sub>12</sub> O <sub>40</sub> , Solvent free, 100 °C, 1 mol%	16	92	34
3	H <sub>2</sub> SO <sub>4</sub> [bmim][BF <sub>4</sub> ], 80 °C, 15 mol%	30	94	35
4	CAN, Solvent free, 50 °C, 5 mol%	120	94	36
5	Citric acid, Solvent free, 80 °C, 3 mol%	20	92	37
6	MNPs-guanidine, Solvent free, 70 °C, 2.34 mol%	35	93	38
7	[C <sub>4</sub> (min) <sub>2</sub> ](FeCl <sub>4</sub> ) <sub>2</sub> , Solvent free, 100 °C, 20 mol%	10	89	39
8	Fe <sub>3</sub> O <sub>4</sub> @Silica sulfuric acid, Solvent free, 100 °C, 0.075 g	35	88	40
9	Iodine / )))))*, Solvent free, 25-30 °C, 10 mol%	10	92	41
10	Al-SBA-15-TPI/H <sub>6</sub> P <sub>2</sub> W <sub>18</sub> O <sub>62</sub> , Solvent free, 100 °C, 0.02g	5	82	This work

### 3. 6. Synthesis of different phthalazine-triones

The generality of this method was examined using several types of aldehydes. In all cases, the reactions gave the corresponding products in good to excellent yields (Table 6). Although, the nature and electronic properties of aldehydes would affect yield%, the reactions proceeded smoothly and equally well for electron-withdrawing as well as electron-donating substituents on aldehydes to afford the corresponding phthalazine-triones. Moreover, aromatic aldehydes reacted faster and led to higher yields% than their aliphatic counterparts.

**Table 6** Synthesis of different 2H-indazolo[2,1-b]phthalazine-1,6,11(13H)-triones in the presence of Al-SBA-15-TPI/H<sub>6</sub>P<sub>2</sub>W<sub>18</sub>O<sub>62</sub> under solvent-free conditions.



Entry	R <sub>1</sub>	R	Time (min)	Yield (%)	m.p. / lit. m.p. (°C)	Ref.
1	Ph	Me	5	82	205-207/206-208	43
2	4-FPh	Me	20	66	222-224/221-224	39
3	2-OHPh	Me	10	76	185-187/184-188	36
4	3-NO <sub>2</sub> Ph	Me	10	78	269-271/268-271	43
5	4-NO <sub>2</sub> Ph	Me	20	84	223-225/222-225	43
6	2-ClPh	Me	12	78	267-269/266-268	41
7	4-ClPh	Me	20	80	261-263/262-264	43
8	2, 6-Cl <sub>2</sub> Ph	Me	15	75	259-261/260-262	44
9	2-OMePh	Me	20	74	242-243/242-243	45
10	3-OMePh	Me	15	69	207-209/206-208	38
11	3, 4-(OMe) <sub>2</sub> Ph	Me	35	72	186-188/185-186	35
12	3-BrPh	Me	10	79	224-227/224-226	38
13	4-BrPh	Me	15	82	266-267/266-268	41
14	4-isopropylPh	Me	30	74	203-205/204-206	42
15	4-Me-Ph	Me	15	72	225-227/226-228	43
16	(CH <sub>3</sub> ) <sub>2</sub> CH- CH <sub>2</sub> -	Me	60	56	135-137/135-137	43
17	(CH <sub>3</sub> ) <sub>2</sub> CH-	Me	120	52	133-135/132-134	43
18	CH <sub>3</sub> -CH <sub>2</sub> -	Me	65	45	146-148/145-147	43
19	Ph	H	15	74	222-224/223-224	34
20	2, 6-Cl <sub>2</sub> Ph	H	40	67	285-287/>280	44
21	4-Me-Ph	H	25	58	245-246/244-246	38

Yields refer to the isolated pure products. The desired pure products were characterized by comparison of their physical data with those of known compounds.

### 3. 7. Hot filtration test

In order to confirm that the catalytic activity was generated from the conjugated Al-SBA-15-TPI/HPA and not from the leached components (if possible) in the reaction mixture, a hot filtration test was carried out. In this technique, the condensation reaction was performed at 100 °C for 2 min in the presence of the Al-SBA-15-TPI/HPA nanocatalyst. At this stage, yield of the product was 60%. The catalyst was then filtered off under hot conditions, and with the filtrate, which was obtained after separation of the catalyst, the reaction was

continued for another 10 min at the same reaction temperature. However, no corresponding increase in the product yield beyond 60% was observed. This result confirmed the heterogeneous nature of the nanocatalyst and that no leaching of the heteropolyacid occurred during the course of the reaction.

### 3. 8. Reusability and reproducibility of Al-SBA-15-TPI/H<sub>6</sub>P<sub>2</sub>W<sub>18</sub>O<sub>62</sub> nanocatalyst

The reusability of the nanocatalyst was tested in the synthesis of 2,2-dimethyl-13-phenyl-2,3-dihydro-1H-indazolo[2,1-b]phthalazine-4,6,11(13H)-trione, as shown in Fig. 5. The catalyst was recovered after each run, washed three times with ethanol, dried in an oven at 90 °C for 4 h and tested in the subsequent run. The nanocatalyst was tested for 8 runs. It was observed that the catalyst displayed very good reusability. Moreover, to ensure reproducibility of the transformation, repeated typical experiments were carried out under identical reaction conditions. The obtained yields were found to be reproducible within ±2% variation.

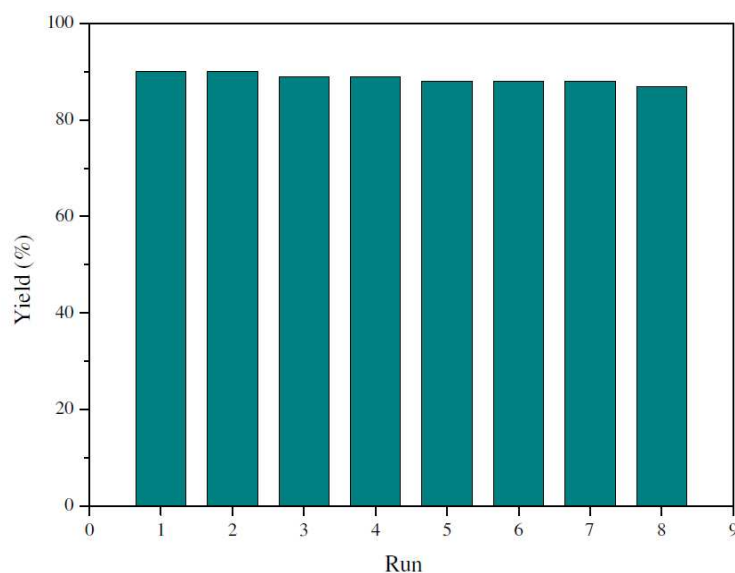
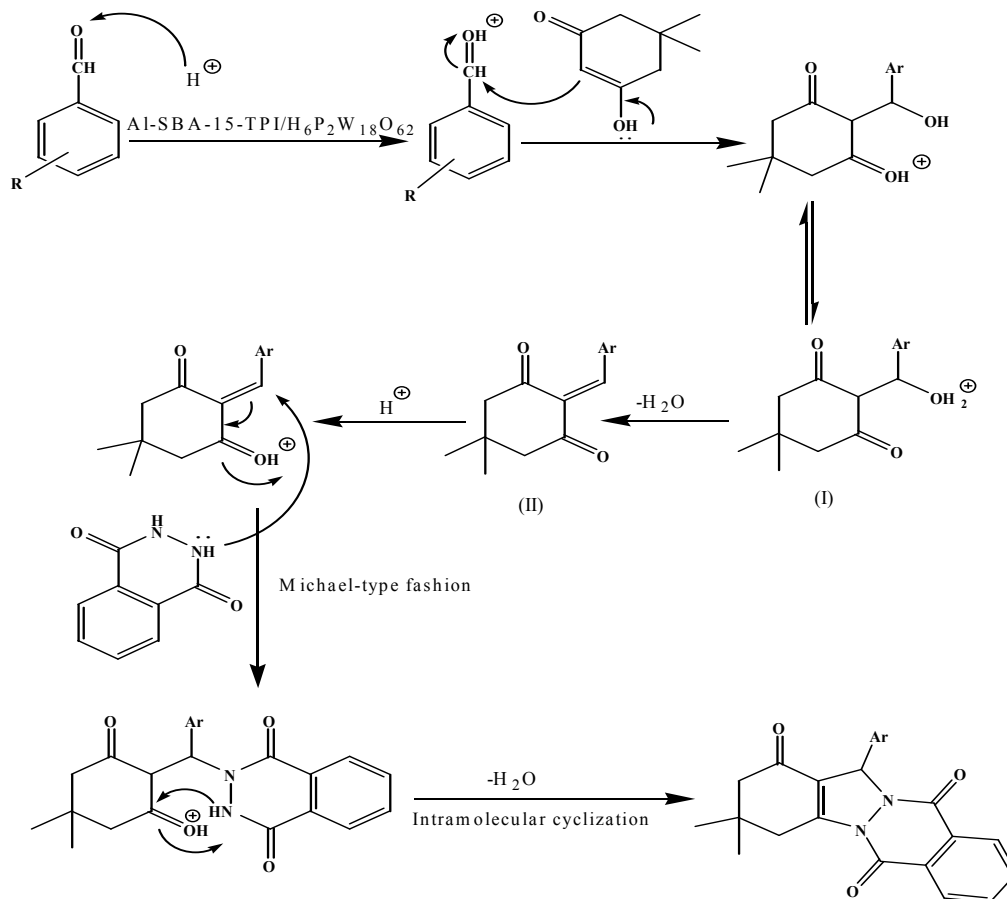


**Fig. 5** Yield% as a function of reusability of Al-SBA-15-TPI/H<sub>6</sub>P<sub>2</sub>W<sub>18</sub>O<sub>62</sub> nanocatalyst.

### 3. 9. Proposed reaction pathway for the heterogeneous catalytic system

A plausible reaction pathway for the reaction of benzaldehyde, phthalhydrazide, and dimedone in the presence of Al-SBA-15-TPI/H<sub>6</sub>P<sub>2</sub>W<sub>18</sub>O<sub>62</sub> nano-hybrid catalyst is presented in Scheme 3. It seems that the reaction starts by *Knoevenagel* condensation of 1,3-dione and aldehyde, followed by *Michael* addition of the phthalhydrazide, and subsequent cyclization to afford the product. It is conceivable that H<sup>+</sup> from the heteropolyacid first bound to the

carbonyl oxygen of the aromatic aldehyde and increased its *Lewis* acidity. Then, nucleophilic addition of dimedone to the carbonyl group of aldehyde led to the generation of (I) and followed by loss of H<sub>2</sub>O afforded (II). As reported in the literature, the *Knoevenagel* type coupling of arylaldehyde with active methylene compounds such as dimedone gives 2-benzylidene-5,5-dimethylcyclohexane-1,3-dione.<sup>46-48</sup> Therefore, subsequent 1,4-conjugate *Michael*-type addition of phthalhydrazide to the olefin followed by cyclization affords the corresponding product.



**Scheme 3** Proposed mechanism for the synthesis of 2*H*-indazolo[1,2-*b*]phthalazine-triones.

#### 4. Conclusion

In summary, a new inorganic-organic nanohybrid material Al-SBA-15-TPI/H<sub>6</sub>P<sub>2</sub>W<sub>18</sub>O<sub>62</sub> was fabricated and used as an efficient catalyst for the one-pot preparation of 2*H*-indazolo[2,1-*b*]phthalazine-1,6,11(13*H*)-trione derivatives from the three-component condensation reaction of phthalhydrazide, dimedone, and aromatic aldehydes. The catalyst was fully

characterized and the catalytic reactions were carried out under thermal solvent free conditions in short times. Furthermore, the catalyst could be successfully recovered and reused at least for eight runs without significant loss of activity. The one-pot nature and the use of heterogeneous solid acid material as an eco-friendly catalyst make the present protocol an interesting alternative to multi-step approaches. This methodology offers significant improvements with regard to the heterogeneous nature of the catalyst, scope of the transformation, simplicity in operation and work up.

### Acknowledgements

Partial financial support from the Research Councils of Hakim Sabzevari and Shahid Beheshti Universities is greatly appreciated.

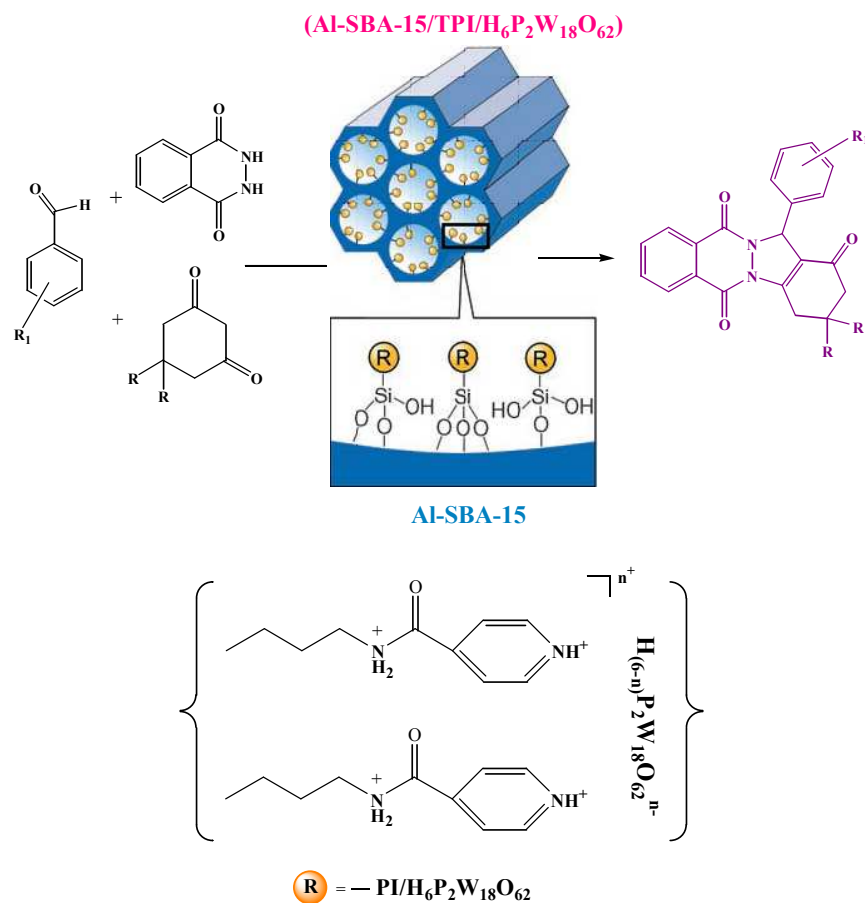
### References

- 1 P. Gómez-Romero, M. Chojak, K. Cuentas-Gallegos, J. A. Asensio, P. J. Kulesza, N. Casañ-Pastor and M. Lira-Cantú, *Electrochem. commun.*, 2003, **5**, 146.
- 2 B. J. Melde, B. T. Holland, C. F. Blanford and A. Stein, *Chem. Mater.*, 1999, **11**, 3302.
- 3 R. Tayebee, M. M. Amini, F. Nehzat, O. Sadeghi and M. Armaghan, *J. Mol. Catal. A: Chem.*, 2013, **366**, 140.
- 4 R. Tayebee, M. M. Amini, N. Abdollahi, A. Aliakbari, S. Rabiei and H. Ramshini, *Appl. Catal., A*, 2013, **468**, 75.
- 5 M. Sayyafi, M. Seyyedhamzeh, H. R. Khavasi and A. Bazgir, *Tetrahedron* 2008, **64**, 2375.
- 6 J. S. Kim, H. J. Lee, M. E. Suh, H. Y. P. Choo, S. K. Lee, H. J. Park, C. Kim, S. W. Park and C. O. Lee, *Bioorg. Med. Chem.*, 2004, **12**, 3683.
- 7 Y. Imamura, A. Noda, T. Imamura, Y. Ono, T. Okawara and H. Noda, *Life Sci.*, 2003, **74**, 29.
- 8 Y. K. Ramtohum, M. N. G. James and J. C. Vederas, *J. Org. Chem.*, 2002, **67**, 3169.
- 9 L. P. Liu, J. M. Lu and M. Shi, *Org. Lett.*, 2007, **9**, 1303.
- 10 R. Ghahremanzadeh, G. I. Shakibaei and A. Bazgir, *Synlett.*, 2008, **8**, 1129.
- 11 R. Tayebee, N. Abdollahi and M. Ghadamgahi, *J. Chin. Chem. Soc.*, 2013, **60**, 1014.
- 12 R. Tayebee, E. Rezaei Seresht, F. Jafari and S. Rabiei, *Ind. Eng. Chem. Res.*, 2013, **52**, 11001.
- 13 R. Tayebee and B. Maleki, *J. Chem. Sci.*, 2013, **125**, 335.
- 14 H. Adkins and F. W. Cox, *J. Am. Chem. Soc.*, 1938, **60**, 1151.
- 15 G. Baronetti, L. Briand, U. Sedran and H. Thomas, *Appl. Catal., A*, 1998, **173**, 265.

- 16 F. Hoffmann, M. Cornelius, J. Morell and M. Froeba, *Angew. Chem. Int.*, 2006, **45**, 3216.
- 17 Y. Wan and D. Zhao, *Chem. Rev.*, 2007, **107**, 2821.
- 18 S. Wu, Y. Han, Y. C. Zou, J. W. Song, L. Zhao, Y. Di, S. Z. Liu and F. S. Xiao, *Chem. Mater.*, 2004, **16**, 486.
- 19 W. Hu, Q. Luo, Y. C. Su, A. M. Zheng, Y. Yue, C. H. Ye and F. Deng, *Micropor. Mesopor. Mater.*, 2006, **92**, 22.
- 20 Y. Li, W. H. Zhang, L. Zhang, Q. H. Yang, Z. B. Wei, Z. C. Feng and C. Li, *J. Phys. Chem. B*, 2004, **108**, 9739.
- 21 R. Van Grieken, J. M. Escola, J. Moreno and R. Rodriguez, *Chem. Eng. J.*, 2009, **155**, 442.
- 22 Q. Yuan, N. Li, Y. Chi, W. C. Geng, W. F. Yan, Y. Zhao, X. T. Li and B. Dong, *Adv. Mater. Res.*, 2013, **254**, 157.
- 23 R. Tayebee, M. M. Amini, M. Ghadamgahi and M. Armaghan, *J. Mol. Catal. A: Chem.*, 2013, **366**, 266.
- 24 S. Ernest and M. Selle, *Micropor. Mesopor. Mater.*, 1999, **27**, 335.
- 25 A. Tarlani, M. Abedini, A. Nemat, M. Khabaz and M. M. Amini, *J. Colloid Interface Sci.*, 2006, **303**, 32.
- 26 R. Tayebee, M. M. Amini, H. Rostamian and A. Aliakbari, *Dalton Trans.*, 2014, **43**, 1550.
- 27 O. Sadeghi, M. M. Amini, M. Feiz Bakhsh Bazargani, A. Mehrani, A. Aghabali, M. Adineh, V. Amani and Kh. Mehrani, *J. Inorg. Organomet. Polym.*, 2012, **22**, 530.
- 28 P. Innocenzi, *J. Non-Cryst. Solids.*, 2003, **316**, 309.
- 29 J. Gong, X. -D. Li, C. -L. Shao, B. Ding, D. -R. Lee and H. -Y. Kim, *Mater. Chem. Phys.*, 2003, **79**, 87.
- 30 E. Ruijter, R. Scheffelaar and R. V. A. Orru, *Angew. Chem. Int. Ed.*, 2011, **50**, 6234.
- 31 R. Tayebee, F. Nehzat, E. Rezaei-Seresht, F. Z. Mohammadi and E. Rafiee, *J. Mol. Catal. A: Chem.*, 2011, **351**, 154.
- 32 P. Karandikar, K. C. Dhanya, S. Deshpande, A. J. Chandwadkar, S. Sivasanker and M. Agashe, *Catal. Commun.*, 2004, **5**, 69.
- 33 A. R. Kiasat, A. Mouradzadegun and J. S. Saghanezhad, *J. Serb. Chem. Soc.*, 2013, **78**, 469.
- 34 H. J. Wang, X. N. Zhang and Z. H. Zhang, *Monatsh. Chem.*, 2010, **141**, 425.
- 35 J. M. Khurana and D. Magoo, *Tetrahedron Lett.*, 2009, **50**, 7300.

- 36 M. Kidwai, R. Chauhan and A. Jahan, *Chin. Sci. Bull.*, 2012, **57**, 2273.
- 37 M. A. Zolfigol, M. Mokhlesi and S. Farahmand, *J. Iran. Chem. Soc.*, 2013, **10**, 577.
- 38 B. Atashkar, A. Rostami, H. Gholami and B. Tahmasbi, *Res. Chem. Intermed.*, 2013, **1**.
- 39 B. M. Godajdar, A. R. Kiasat and M. M. Hashemi, *Heterocycles.*, 2013, **87**, 559.
- 40 A. R. Kiasat and J. Davarpanah, *J. Mol. Catal. A: Chem.*, 2013, **373**, 46.
- 41 A. Varghese, A. Nizam, R. Kulkarni and L. George, *Eur. J. Chem.*, 2013, **4**, 132.
- 42 G. Sabitha, C. Srinivas, A. Raghavendar and J. S. Yadav, *Helv. Chim. Acta.*, 2010, **93**, 1375.
- 43 R. G. Vaghei, R. K. Nami, Z. T. Semiromi, M. Amiri and M. Ghavidel, *Tetrahedron* 2011, **67**, 1930.
- 44 A. Hasaninejad, M. R. Kazerooni and A. Zare, *Catal. Today.*, 2012, **196**, 148.
- 45 M. Shekouhy and A. Hasaninejad, *Ultrason. Sonochem.*, 2012, **19**, 307.
- 46 A. Kumar and R. A. Maurya, *Tetrahedron* 2007, **63**, 1946.
- 47 G. Kaupp, M. R. Naimi-Jamal and J. Schmeyers, *Tetrahedron* 2003, **59**, 3753.
- 48 J. Quiroga, D. Mejía, B. Insuasty, R. Abonía, M. Noguera, A. Sánchez, J. Cobo and J. N. Low, *Tetrahedron* 2001, **57**, 6947.

## Graphical Abstract



Al-SBA-15-TPI/H<sub>6</sub>P<sub>2</sub>W<sub>18</sub>O<sub>62</sub> is introduced as an effective catalyst for the one-pot synthesis of indazolo-phthalazine-triones. The catalyst could be easily separated without noticeable reduction in activity.